PCCP

RSC Publishing

PAPER

View Article Online
View Journal | View Issue

Trimetallic deltahedral Zintl ions $[Sn_{9-m-n}Ge_mBi_n]^{(4-n)-}$ for n = 1–4 and m = 0–(9 − n): a theoretical survey with prediction and rationalization of the possible structures†

Cite this: *Phys. Chem. Chem. Phys.*, 2013, **15**, 986

Alvaro Muñoz-Castro*[a] and Slavi C. Sevov*[b]

Received 11th September 2012,
Accepted 16th November 2012

DOI: 10.1039/c2cp43196c

www.rsc.org/pccp

The recent discovery of trimetallic deltahedral Zintl ions based on Sn, Ge, and Bi revealed the possibility to obtain such clusters with a variety of different Sn/Ge/Bi ratios. Although only the dimer $[(BiSn_6Ge_2)–(Ge_2Sn_6Bi)]^{4-}$ was structurally characterized, a number of other nine-atom clusters with various stoichiometries were detected by electrospray mass spectrometry. The lack of structural data for the latter persuaded us to use relativistic density functional calculations in order to determine and rationalize theoretically the most stable structure conformation of each cluster and the positional preferences for the different atoms in the series $[Sn_{9-m-n}Ge_mBi_n]^{(4-n)-}$ where n = 1–4 and m = 0–(9 − n). The analysis revealed strong dependence of the cluster geometry on the cluster stoichiometry and revealed sites with significantly different charge distribution. In addition, we introduce a parameter ϕ based on certain angles in order to rationalize the obtained structures as monocapped square antiprisms (C_{4v}), tricapped trigonal prisms (D_{3h}), or intermediates (C_{2v}).

Introduction

The nine-atom deltahedral Zintl ions of group 14 and their chemistry have experienced renewed interest during the past decade, mainly due to their unusual reactivity and formation of novel compounds.[1] One of the major discoveries was the functionalization of the Zintl ions by reactions with organic halides RX, alkynes RC≡CR, and main-group organometallic halides R_3EX for group 14 and R_2EX for group 15.[1–5] Until very recently, the maximum number of external substituents at the clusters was thought to be two. However, it was shown in the last few months that reactions of Ge_9^{4-} clusters with $(Me_3Si)_3SiCl$ in appropriate solvents result in the tri-substituted $[Ge_9\{Si(SiMe_3)_3\}_3]^-$ monoanion.[2d] Furthermore, subsequent reaction of the latter with Ph_3SnCl resulted in the tetrasubstituted and neutral $[Ge_9\{Si(SiMe_3)_3\}_3\{SnPh_3\}]^0$ (ref. 6) which is soluble in several nonpolar organic solvents, thus providing many possibilities for expanding the chemistry of the functionalized clusters to further explorations.

One way to diversify further this unique and interesting chemistry observed for homoatomic clusters is to apply it to analogous and isoelectronic heteroatomic species. The great potential given by the inherent capabilities to obtain intermetallic precursors with various nominal compositions[7] by high-temperature reactions provides almost endless potential possibilities to vary the stoichiometry of the extracted heteroatomic clusters.[8,9] In addition, this potential versatility is supplemented by the heteroatomic clusters' ability to be functionalized with various *exo*-bonded groups.[3] Lastly, it has been shown that, upon heating, homoatomic Ge_9 clusters functionalized with group 15 fragments such as Ph_2Sb– and Ph_2Bi– exchange Ge-atoms from the cluster for Sb or Bi from the fragments to also produce nine-atom heteroatomic clusters and dimers such as $[Sb_2Ge_7]^{2-}$, $[(SbGe_8)_2]^{4-}$, and $[(BiGe_8)_2]^{4-}$.[10] In pursuit of expanding the library of heterometallic deltahedral Zintl ions, we have carried out similar extractions of clusters from even more complex precursors, namely quaternary intermetallics made of K, Sn, Ge, and Bi. We recently reported the synthesis and structure of the first tri-metallic deltahedral Zintl ions in the dimer $[(BiSn_6Ge_2)–(Ge_2Sn_6Bi)]^{4-}$ extracted from a precursor with a nominal composition "$K_4Sn_4Ge_4Bi$".[11] More importantly, however, the electrospray mass spectrum (ES-MS) of the dissolved precursor showed a number of additional nine-atom

[a] *Departamento de Ciencias Quimicas, Universidad Andres Bello, Av. Republica 275, Santiago, Chile. E-mail: alvaro.munoz@unab.cl; Fax: +56 02-770-3352; Tel: +56 02-661-8249*

[b] *Department of Chemistry and Biochemistry, University of Notre Dame, Notre Dame, Indiana 46556, USA. E-mail: ssevov@nd.edu; Fax: +1 574-631-6652; Tel: +1 574-631-5891*

† Electronic supplementary information (ESI) available. See DOI: 10.1039/c2cp43196c

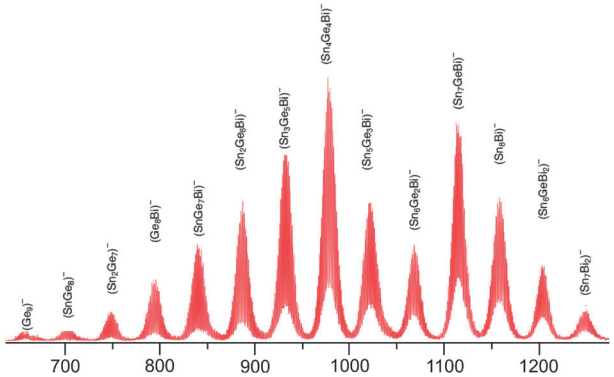

Fig. 1 The ES-mass spectrum of an ethylenediamine solution of an intermetallic precursor with nominal composition "$K_4Sn_4Ge_4Bi$".[11]

species as well (Fig. 1), some with one and some with two Bi-atoms. Although they all show as species with a charge of 1− in the spectrum as typically observed for nine-atom clusters (a result of the oxidation of the parent polyanion by the cone voltage during the course of the measurement), they are most likely isoelectronic with the well known E_9^{4-} clusters for E = Si, Ge, Sn, Pb. The cluster-bonding electron count of the latter, $2n + 4 = 22$ for $n = 9$, classifies them as *nido*-clusters that, ideally, should be monocapped square antiprisms (msa) with C_{4v} symmetry. In reality, though, they are known to exhibit inherent fluxional behavior often deviating greatly from C_{4v} towards distorted tricapped trigonal prismatic (ttp) shape with pseudo-D_{3h} symmetry and elongated one, two, or all three prismatic edges parallel to the three-fold axis.[11,12] It should be pointed out that the msa geometry can be viewed as one specific case of distortion of ttp such that only one edge is elongated so much that it becomes a diagonal in a open square face (C_{4v} symmetry). The degree of elongation in the cases of elongated two and three edges becomes progressively smaller and the corresponding pairs of atoms retain some degrees of interaction (and connecting lines are often drawn in the structures). The resulting structures are close to C_{2v} and again D_{3h} symmetry, respectively.

All the above factors make the prediction of the cluster geometry a difficult task which becomes even more difficult for the corresponding tri-metallic derivatives. Added to the complexity in the latter cases are the multiple possibilities for positioning the constituent elements at the nine vertices. We report here our results on predicting the conformations of such nine-atom Sn–Ge–Bi deltahedral Zintl ions containing up to the possible maximum of four Bi atoms (beyond that the clusters become cationic and much less likely to exist under the particular experimental conditions) in order to expand the understanding of the potential reactivity of such heteroatomic species.

Computational details

Relativistic DFT calculations were carried out in order to determine the preferred structures and element distributions of the trimetallic nine-atom clusters $[Sn_{9-m-n}Ge_mBi_n]^{(4-n)-}$ for n = 1–4 and m = 0–(9 − n). Employed was the ADF 2010.01 code[13] with the triple-ξ Slater basis set plus the double polarization (STO-TZ2P) basis set in conjunction with the non-local Perdew–Burke–Ernzerhof (PBE) functional within the generalized gradient approximation (GGA).[14] Relativistic effects were taken into account by ZORA formalism[15] using two-component wavefunctions, including both scalar and spin–orbit coupling, consistent with our previous studies on metallic clusters.[16] Evaluated initially were all possible arrangements of the constituent elements in the nine-atom clusters for the different stoichiometries. This was done in the frozen core approximation with inner shells of [$1s^2$–$3d^{10}$] for Ge, [$1s^2$–$4d^{10}$] for Sn, and [$1s^2$–$5d^{10}$] for Bi. The convergence criteria were fixed at 10^{-5} hartree for the energy and at 10^{-4} hartree $Å^{-1}$ for the energy gradient in the geometry optimization. The nature of each optimized stationary point on the potential energy surface (PES) was determined by examining the second derivative of the energy with respect to the coordinates (Hessian). Then the low-lying conformations were reoptimized in all-electron basis sets using a tighter optimization criteria fixed to 10^{-7} hartree and 10^{-6} hartree $Å^{-1}$ for the energy and energy gradient, respectively, and to 0.01 degree for angles. The total bonding energies of the structures discussed here are all obtained at the former level of theory. Charge distribution calculations were performed at the scalar relativistic level (scalar/ZORA) by means of natural bond orbital (NBO) analysis implemented in the stand-alone NBO5 suite.[17]

Results and discussion

The ES-MS of the quaternary precursor "$K_4Sn_4Ge_4Bi$" dissolved in ethylenediamine (Fig. 1) shows all possible nine-atom clusters with one Bi-atom and eight Sn/Ge-atoms, *i.e.* $[Sn_{8-m}Ge_mBi]^{3-}$ for m = 0–8, as well as a couple of clusters with two Bi-atoms, namely $[Sn_6GeBi_2]^{2-}$ and $[Sn_7Bi_2]^{2-}$.[11] The structurally characterized dimer $[(Sn_6Ge_2Bi)_2]^{4-}$ is in essence the oxidatively coupled pair of $[Sn_6Ge_2Bi]^{3-}$ clusters with a Ge–Ge intercluster bond. The positioning of the two Ge and one Bi '*heteroatoms*' in the latter cluster has already been theoretically evaluated in an imaginary process of replacing Sn-atoms in a homoatomic $[Sn_9]^{4-}$.[11] It was predicted and experimentally confirmed by single-crystal X-ray diffraction data that the three heteroatoms cap the three rectangular faces of a 'Sn_6' trigonal prism.[11] The overall optimized structure of the $[Sn_6Ge_2Bi]^{3-}$ monomer was found to be very close to a pseudo-D_{3h} tricapped trigonal prism. The observed shape of the clusters within the dimer is also very close to that.

This observed capability of the Sn/Ge clusters to incorporate one and two bismuth atoms encouraged us to predict and rationalize the possible structures of the resulting deltahedral clusters in the isoelectronic series $[Sn_{9-m-n}Ge_mBi_n]^{(4-n)-}$ for n = 1–4 and m = 0–(9 − n), *i.e.* all the way up to neutral species with four bismuth atoms. In order to elucidate the favored structure for each composition we carried out an extensive evaluation of the possible structural and positional conformers by considering all the possible starting points of a nine-vertex aggregate for the different stoichiometries. The already mentioned observed fluxionality of the clusters between

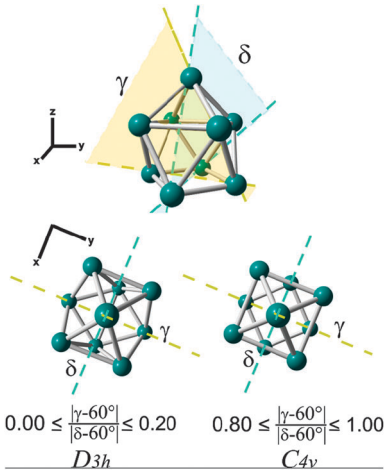

Fig. 2 Definition of the angles γ and δ in a nine-atom cluster where always $\gamma \geq \delta$.

idealized C_{4v} and D_{3h} symmetry means that they had to be considered starting from both msa and ttp conformations.[12]

In order to rationalize, compare, and classify the resulting structures as C_{4v}, D_{3h}, or neither, which is typically close to C_{2v}, we focused on the ratio between certain angles in the cluster instead on the previously used interatomic distances. The reason is that the latter depend much more on the sizes of the atoms, and this makes them less useful when three different elements are involved. For our classification purposes we view the cluster initially as a monocapped square antiprism and use the two angles γ and δ that each diagonal of the uncapped square forms with the atom capping the capped square of the antiprism (Fig. 2). If the two diagonals are different, then γ is the angle that corresponds to the longer one. We then take the absolute values of the deviations of these angles from 60° and define ϕ as their ratio, *i.e.* $\phi = |\gamma - 60^\circ|/|\delta - 60^\circ|$ with $|\gamma - 60^\circ| < |\delta - 60^\circ|$. Thus, in an ideal tricapped trigonal prism with D_{3h} symmetry the three capping atoms form an equilateral triangle with $\gamma = 60^\circ$ and, therefore, $\phi = 0$. On the other hand, in an ideal monocapped square antiprism with C_{4v} symmetry $\gamma = \delta$ ($<60^\circ$) and, therefore, $\phi = 1$. In our evaluation of the preferred theoretically derived conformations we have assigned the corresponding idealized geometry if ϕ for the calculated conformation does not deviate by more than 20% from ϕ for the idealized geometry, *i.e.* D_{3h} is assigned for calculated ϕ = 0–0.2 while C_{4v} is assigned for ϕ = 0.8–1.0. The structures that fall in between these ranges are all pseudo-C_{2v} and they have been assigned as such.

The results from the calculations, *i.e.* the conformational and positional global minima for $[Sn_mGe_{9-m-n}Bi_n]^{(4-n)-}$, are presented in Table 1 and Fig. 3–6, while the corresponding total bonding energies are provided in the ESI† (Table S1). There are a few general observations common for all the clusters. First, the electron-richest element of the three, bismuth, occupies consistently positions with the lowest possible connectivity which is four in this case. This has been observed before in $[In_4Bi_5]^{3-}$ with a msa geometry where the five bismuth atoms occupy all available four-connected positions, *i.e.* the capping

Table 1 Calculated parameters and predicted structures for the most stable clusters in the series $[Sn_{9-m-n}Ge_mBi_n]^{(4-n)-}$ for n = 1–4 and m = 0–(9 − n)

Composition	$\lvert\gamma - 60^\circ\rvert$	$\lvert\delta - 60^\circ\rvert$	ϕ	Symmetry
$[Ge_8Bi]^{3-}$	1.2	11.5	0.10	$\sim D_{3h}$
$[SnGe_7Bi]^{3-}$	3.1	3.1	1.00	C_{4v}
$[Sn_2Ge_6Bi]^{3-}$	3.6	7.2	0.50	$\sim C_{2v}$
$[Sn_3Ge_5Bi]^{3-}$	0.8	16.1	0.05	D_{3h}
$[Sn_4Ge_4Bi]^{3-}$	1.5	24.6	0.06	D_{3h}
$[Sn_5Ge_3Bi]^{3-}$	0.3	22.9	0.01	D_{3h}
$[Sn_6Ge_2Bi]^{3-}$	0.7	10.8	0.06	D_{3h}
$[Sn_7GeBi]^{3-}$	3.8	3.9	0.97	C_{4v}
$[Sn_8Bi]^{3-}$	2.4	10.4	0.23	$\sim D_{3h}$
$[Ge_7Bi_2]^{2-}$	2.5	6.3	0.40	$\sim C_{2v}$
$[SnGe_6Bi_2]^{2-}$	2.5	3.5	0.71	$\sim C_{2v}$
$[Sn_2Ge_5Bi_2]^{2-}$	1.6	1.8	0.89	$\sim C_{4v}$
$[Sn_3Ge_4Bi_2]^{2-}$	3.1	6.3	0.49	$\sim C_{2v}$
$[Sn_4Ge_3Bi_2]^{2-}$	4.2	4.2	1.00	C_{4v}
$[Sn_5Ge_2Bi_2]^{2-}$	4.9	4.7	0.96	C_{4v}
$[Sn_6Ge_1Bi_2]^{2-}$	5.5	5.6	0.98	C_{4v}
$[Sn_7Bi_2]^{2-}$	7.7	7.8	0.99	C_{4v}
$[Ge_6Bi_3]^{-}$	2.4	2.5	0.96	C_{4v}
$[SnGe_5Bi_3]^{-}$	1.8	3.8	0.47	$\sim C_{2v}$
$[Sn_2Ge_4Bi_3]^{-}$	1.7	2.9	0.59	$\sim C_{2v}$
$[Sn_3Ge_3Bi_3]^{-}$	2.1	3.1	0.68	$\sim C_{2v}$
$[Sn_4Ge_2Bi_3]^{-}$	2.6	3.2	0.81	$\sim C_{4v}$
$[Sn_5GeBi_3]^{-}$	5.5	5.7	0.96	C_{4v}
$[Sn_6Bi_3]^{-}$	0.0	7.0	0.00	D_{3h}
$[Ge_5Bi_4]$	1.5	1.6	0.93	C_{4v}
$[SnGe_4Bi_4]$	2.3	2.4	0.96	C_{4v}
$[Sn_2Ge_3Bi_4]$	2.0	4.1	0.49	$\sim C_{2v}$
$[Sn_3Ge_2Bi_4]$	3.4	3.5	0.97	C_{4v}
$[Sn_4GeBi_4]$	2.8	2.8	1.00	C_{4v}
$[Sn_5Bi_4]$	2.9	5.2	0.58	$\sim C_{2v}$

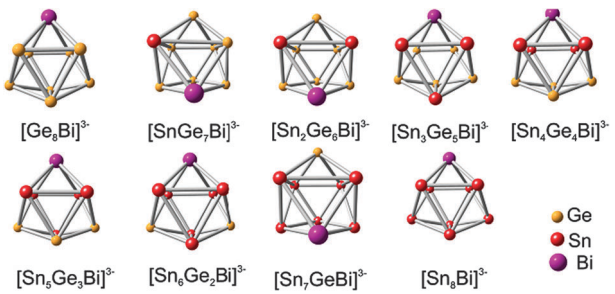

Fig. 3 Global minima structures for $[Sn_{8-m}Ge_mBi]^{3-}$ (m = 0–8).

vertex and the four vertices forming the uncapped square face. According to several theoretical calculations on E_9^{4-} clusters (E = group 14 element) utilizing a variety of methods, the four-bonded positions carry higher negative charges than the five-bonded ones and are, therefore, preferred by electron-richer elements.[18]

Another general observation is that germanium prefers capping positions, *i.e.* the position capping the square in msa or one of the three capping positions in ttp (it caps distorted square in the intermediate C_{2v}). Such positions are also four-connected and, as already discussed above, carry higher negative charge. Therefore, when the choice is between Ge and Sn, it is logical to expect that the slightly more electronegative Ge will take such a position.

The preference for four-connected positions for Bi and Ge leaves the Sn-atoms to occupy preferentially the five-connected

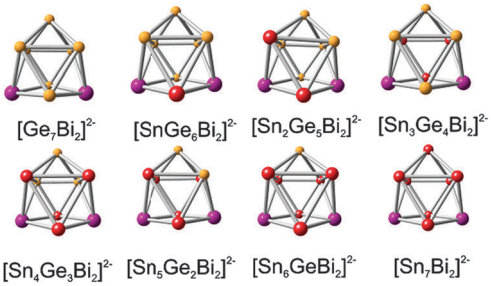

Fig. 4 Global minima structures for $[Sn_{7-m}Ge_mBi_2]^{2-}$ (m = 0–7).

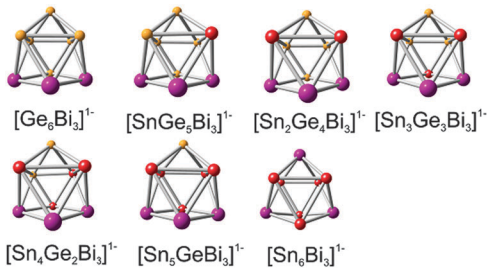

Fig. 5 Global minima structures for $[Sn_{6-m}Ge_mBi_3]^{1-}$ (m = 0–6).

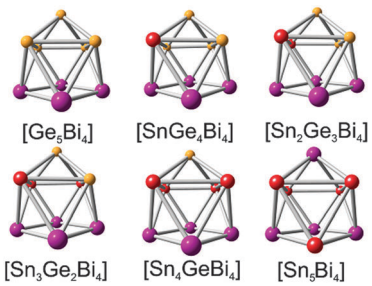

Fig. 6 Global minima structures for $[Sn_{6-m}Ge_mBi_4]^0$ (m = 0–5).

positions. This is clearly visible in the first series with one Bi-atom shown in Fig. 3. Furthermore, the experimentally determined structure of $[(Sn_6Ge_2Bi)_2]^{4-}$ confirms exactly the theoretically predicted geometry and atomic positions for at least one member of the series. Notice that all six Sn-atoms occupy 5-connected positions while the two Ge- and one Bi-atoms take the three 4-connected positions in this slightly elongated ttp geometry.

The energies of the isomers closest to the global minima structures were calculated as well (Fig. S3–S6 in ESI†). It is noticed that these low-energy isomers are only less than 1 kcal mol^{-1} away from global minima with intermediate ϕ values and thus pseudo-C_{2v} symmetry. This suggests that these intermediate geometries have other possible conformations at accessible energy levels. In addition, three cases with almost perfectly defined geometries, namely $[Sn_5Ge_3Bi]^{3-}$ (ϕ = 0.01), $[Sn_5Ge_2Bi_2]^{2-}$ (ϕ = 0.96), and $[Sn_4Ge_3Bi_2]^{2-}$ (ϕ = 1.00) also have conformations lying at less than 1 kcal mol^{-1} above the global minima. In terms of ϕ values and therefore geometries, all these low-energy conformations are close to the corresponding parent global-minima conformations. This suggests that the observed trends for the latter can be extended and are valid also for the low-energy conformations lying within 1 kcal mol^{-1}.

In addition to the above analysis of the low-lying conformations in terms of energy and ϕ values, we also employed the so-called *continuous-shape-measure* (CShM) approach[19] in order to further quantify the departure of a given nine-atom deltahedral Zintl ion from a perfect msa or ttp polyhedron (Table S2 in ESI†). The calculated deviations agree very well with the corresponding ϕ values, thus supporting further the assignments of pseudo-C_{4v} or -D_{3h} geometries as well as the intermediate C_{2v} cases.

By comparing the charge distributions among the atoms of Ge_9^{4-} and Sn_9^{4-} with the msa or ttp geometry (see ESI†), it is possible to observe the variation of the electron-rich/-poor sites when changing the shape of the cluster from msa to ttp. As discussed above, the msa has five four-connected and four five-connected positions (correspondingly the open square plus the capping site on one hand and the capped square on the other) and, therefore, can readily accommodate five more electronegative and four less electronegative atoms. In contrast, the regular ttp geometry, *i.e.* with no elongated edges along the three-fold axis, has only three four-connected but six five-connected positions (the capping and the prismatic positions, respectively) which makes it more suitable for heteroatomic clusters with only three atoms of higher electronegativity. Even with the observed small elongations of one or more of the three edges along the three-fold axis, the six prismatic positions remain more or less five-connected. These differences suggest that, in the case of Sn/Ge/Bi trimetallic clusters, the ttp structure should be favored for compositions with fewer Bi-atoms while clusters with more Bi-atoms should prefer the msa geometry. The computational results presented in Table 1 corroborate this observation as most of the clusters with one Bi-atom, *i.e.* $[Sn_mGe_{8-m}Bi]^{3-}$, are with close to D_{3h} symmetry while those with 2–4 Bi-atoms are either C_{4v} or with the intermediate geometry. The structural effect of adding more germanium to replace tin atoms is not as strong most likely because the two elements are not that dissimilar in electronegativity.

Focusing on the Sn-atoms it seems that in all four series they tend to occupy such positions that would bring maximum number of Sn–Sn interactions. Here are some examples: (a) upon going from one to two tin atoms per cluster, the second tin atom takes a position that is connected to the first one in all four series, *i.e.* from $[SnGe_{8-n}Bi_n]^{(4-n)-}$ to $[Sn_2Ge_{7-n}Bi_n]^{(4-n)-}$; (b) upon going from $[Sn_2Ge_{7-n}Bi_n]^{(4-n)-}$ to $[Sn_3Ge_{6-n}Bi_n]^{(4-n)-}$, the three tin atoms form a triangle in the first two series and a chain in the fourth one; (c) upon going from $[Sn_3Ge_{6-n}Bi_n]^{(4-n)-}$ to $[Sn_4Ge_{5-n}Bi_n]^{(4-n)-}$ the four tin atoms form a square in the first and fourth series and a chain in the third one. Yet another pattern is the tendency of the tin atoms to bond to bismuth atoms. This is clearly visible in the second series where there is always at least one tin atom bonded to both bismuth atoms. This is also a very strong trend in the remaining three series.

Taking a closer look at each series, we see that in the first one D_{3h} is the preferred geometry (Table 1 and Fig. 3). Notice how close to this geometry is the calculated ratio ϕ = 0.06 for the structurally determined cluster $[(Sn_6Ge_2Bi)_2]^{4-}$. For comparison, the ratio for the experimentally observed structure is ϕ = 0.08. Similarly, very close to ideal D_{3h} are the three compositions preceding the observed one, *i.e.* $[Sn_mGe_{8-m}Bi]^{3-}$ for m = 3–5 with ϕ = 0.01–0.06. The two end members $[Ge_8Bi]^{3-}$ and $[Sn_8Bi]^{3-}$ can also be described confidently as close to D_{3h} with ϕ = 0.10 and 0.23, respectively, although slightly more deviated from it than the previously described four members. At the same time, the two isomers next to each of the two end members, *i.e.* the one with a single Sn-atom and the one with a single Ge-atom, are with almost perfect C_{4v} symmetry with ϕ = 1.00 and 0.97, respectively. Lastly, $[Sn_2Ge_6Bi]^{3-}$ provides an interesting case with ϕ = 0.50 thus being half way between the two extremes and has overall C_{2v} symmetry.

The inclusion of a second Bi-atom in the trimetallic clusters (Fig. 4) changes the overall preferred geometry from mostly D_{3h} to predominantly C_{4v} and the intermediate C_{2v} as suggested by the range of 0.40–1.00 for the ϕ parameter (Table 1). In the entire series, the two Bi-atoms take two diagonally opposed vertices in the open *pseudo* square face, specifically those at the shorter diagonal which corresponds to the δ angle. It should be pointed out that our predicted bismuth positions and C_{4v} geometry for the $[Sn_7Bi_2]^{2-}$ end member of this series are in excellent agreement with the previously reported results based on DFT BP86/def2-TZVP level calculations.[19] Furthermore, the two calculations agree also on the closest-lying isomer, calculated to be with a Bi–Bi bond, retaining the C_{4v} geometry (ϕ = 0.99), and at about 4.54 kcal mol^{-1} above the minimum (4.39 kcal mol^{-1} reported before,[20] ESI†).

The series with three Bi-atoms exhibits an interesting continuous variation of the cluster shapes. Excluding the two end members, the shape indicator ϕ increases gradually from 0.47 to 0.96 upon replacing more Ge- with Sn-atoms (Table 1 and Fig. 5). This means that the clusters go from very highly distorted to almost perfect C_{4v} shape. The shapes of the two end members, on the other hand, are exactly opposite to this trend, namely C_{4v} for $[Ge_6Bi_3]^-$ which is next to the most C_{2v}-distorted $[SnGe_5Bi_3]^-$ and D_{3h} for $[Sn_6Bi_3]^-$ which is next to $[Sn_6GeBi_3]^-$ with almost perfect C_{4v} symmetry. Notice that the Sn/Bi end member is the only member of the series without Bi–Bi interactions in a Bi–Bi–Bi fragment, although the isomer with such a fragment is fairly close to C_{4v} (ϕ = 0.81) and is energetically the closest to the minimized shape at about 3.02 kcal mol^{-1} (ESI†). One possible reason for the diametrically different shapes of the two end members might be the larger electronegativity difference for the Sn/Bi pair compared to the Ge/Bi pair and the resulting greater difference in preferences for positions with different connectivity. Another possible reason might be the order of preferred interactions for the Bi-atoms which might be Bi–Bi > Bi–Sn > Bi–Ge which would explain the existence of the Bi–Bi–Bi fragment in all but the Sn/Bi end member.

These same reasons are perhaps responsible for a similar observation in the series with four Bi-atoms (Fig. 6 and Table 1) where all but the Sn/Bi end member exhibit a square of Bi-atoms, although the isomer with a Bi-square for the latter is fairly close in energy at only 0.45 kcal mol^{-1} from the minimum. Notice that the positions taken by the Sn-atoms in the gradual replacement of Ge-atoms are always five-connected (electronegativity differences) and are the closest to the Bi-atoms (preferred Bi–Sn *vs.* Bi–Ge interactions). Geometry-wise, the only two members deviating greatly from C_{4v} are the Sn/Bi end member and $[Sn_2Ge_3Bi_4]$, both with distorted C_{2v} symmetry.

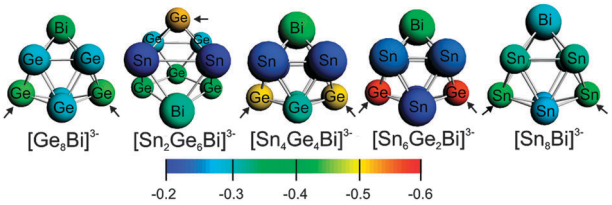

Fig. 7 Natural charge analysis for $[Sn_{8-m}Ge_mBi]^{3-}$ for m = 0, 2, 4, 6, and 8 with arrows denoting the highest charge concentrations in each cluster. Values denote the nuclear charge (Z) minus the total electron population on each nucleus.

Lastly, we also carried out natural charge analysis on every other member of the series with one bismuth atom, *i.e.* $[Sn_{8-m}Ge_mBi]^{3-}$ for m = 0, 2, 4, 6, and 8, in order to gain insight into the charge distribution of what seems to be the most stable clusters according to the mass spectrum. The analysis reveals, as somewhat expected and already briefly discussed, that the charge is concentrated at the four-connected sites (Fig. 7). Viewing the clusters approximately as tricapped trigonal prisms, these sites are the capping positions. In that respect, the charge distribution can be rationalized as the central trigonal prism donating charge towards the capping positions. Also, it seems that the four-connected sites with the highest charge are the most active in external interactions judging from the typical positions of *exo*-bonded groups in the homoatomic Ge_9-clusters and the inter-cluster bond in the observed dimer of $[(Sn_6Ge_2Bi)_2]^{4-}$.[11]

Summary

All possible structures for the series of Sn/Ge/Bi trimetallic nine-vertex deltahedral clusters with 1–4 bismuth atoms and 40 valence electrons were evaluated and global minima were determined in each potential-energy-surface. It is important to point out that the structure predicted for $[Sn_6Ge_2Bi]^{3-}$ using this approach is in excellent agreement with the experimentally characterized species ($[(Sn_6Ge_2Bi)_2]^{4-}$). The obtained structures were categorized as C_{4v}, D_{3h}, or intermediate C_{2v} based on the ratio ϕ between the angles that the two diagonals of the most open square-like face form with the farthest atom. The trends in preferred structures and positional preferences for the three different elements were rationalized.

Acknowledgements

The authors thank the financial support from FONDECYT 11100027, PROJECT MILLENNIUM No. P07-006–F, and from the National Science Foundation (CHE-0742365).

Notes and references

1 (*a*) S. Scharfe and T. F. Flassler, *Philos. Trans. R. Soc. London, Ser. A*, 2010, **368**, 1265; (*b*) E. Zintl and A. Harder, *Z. Phys. Chem., Abt. A*, 1931, **154**, 47; (*c*) J. D. Corbett and P. A. Edwards, *J. Am. Chem. Soc.*, 1977, **99**, 3313; (*d*) J. D. Corbett, *Chem. Rev.*, 1985, **85**, 383; (*e*) A. Ugrinov and S. C. Sevov, *Appl. Organomet. Chem.*, 2003, **17**, 373; (*f*) J. M. Goicoechea and S. C. Sevov, *J. Am. Chem. Soc.*, 2004, **126**, 6860; (*g*) B. Eisenmann, *Angew. Chem., Int. Ed. Engl.*, 1993, **32**, 1693; (*h*) V. Quéneau and S. C. Sevov, *Angew. Chem., Int. Ed. Engl.*, 1997, **36**, 1754; (*i*) V. Quéneau, E. Todorov and S. C. Sevov, *J. Am. Chem. Soc.*, 1998, **120**, 3263; (*j*) E. Todorov and S. C. Sevov, *Inorg. Chem.*, 1998, **37**, 3889; (*k*) S. C. Sevov, in *Intermetallic Compounds, Principles and Practice: Progress*, ed. J. H. Westbrook and R. L. Freisher, John Wiley & Sons. Ltd., Chichester, England, 2002, pp. 113–132; (*l*) S. C. Sevov and J. M. Goicoechea, *Organometallics*, 2006, **25**, 5678.

2 (*a*) M. W. Hull and S. C. Sevov, *Inorg. Chem.*, 2007, **46**, 10953; (*b*) J. M. Goicoechea and S. C. Sevov, *J. Am. Chem. Soc.*, 2006, **128**, 4155; (*c*) D. J. Chapman and S. C. Sevov, *Inorg. Chem.*, 2008, **47**, 6009; (*d*) F. Li and S. C. Sevov, *Inorg. Chem.*, 2012, **51**, 2706; (*e*) A. Schnepf, *Angew. Chem., Int. Ed.*, 2003, **42**, 2624.

3 M. M. Gillett-Kunnath, I. Petrov and S. C. Sevov, *Inorg. Chem.*, 2010, **49**, 721.

4 (*a*) B. Schiemenz and G. Huttner, *Angew. Chem., Int. Ed. Engl.*, 1993, **32**, 295; (*b*) G. Renner, P. Kircher, G. Huttner, P. Rutsch and K. Heinze, *Eur. J. Inorg. Chem.*, 2001, 973; (*c*) B. Kesanli, J. Fettinger and B. Eichhorn, *Chem.–Eur. J.*, 2001, 7, 5277; (*d*) C. Schenk and A. Schnepf, *Dalton Trans.*, 2007, 5400; (*e*) F. Henke, C. Schenk and A. Schnepf, *Dalton Trans.*, 2011, **40**, 6704; (*f*) M. W. Hull and S. C. Sevov, *Angew. Chem., Int. Ed.*, 2007, **46**, 6695.

5 A. Ugrinov and S. C. Sevov, *Chem.–Eur. J.*, 2004, **10**, 3727.

6 F. Li, A. Muñoz-Castro and S. C. Sevov, *Angew. Chem., Int. Ed.*, 2012, **51**, 8581.

7 (*a*) M. M. Gillett-Kunnath, J. I. Paik, S. M. Jensen, J. D. Taylor and S. C. Sevov, *Inorg. Chem.*, 2011, **50**, 11695; (*b*) D. Rios, M. M. Gillett-Kunnath, J. D. Taylor, A. G. Oliver and S. C. Sevov, *Inorg. Chem.*, 2011, **50**, 2373; (*c*) J. M. Goicoechea and S. C. Sevov, *Angew. Chem., Int. Ed.*, 2006, **45**, 5147; (*d*) F. Lips, R. Clerac and S. Dehnen, *Angew. Chem., Int. Ed.*, 2011, **50**, 960; (*e*) F. Lips, R. Clerac and S. Dehnen, *J. Am. Chem. Soc.*, 2011, **133**, 14168.

8 (*a*) J. M. Goicoechea and S. C. Sevov, *Angew. Chem., Int. Ed.*, 2005, **127**, 4026; (*b*) J. M. Goicoechea and S. C. Sevov, *J. Am. Chem. Soc.*, 2005, **127**, 7676; (*c*) E. N. Esenturk, J. Fettinger and B. W. Eichhorn, *J. Chem. Soc., Chem. Commun.*, 2005, 247; (*d*) E. N. Esenturk, J. Fettinger and B. W. Eichhorn, *J. Am. Chem. Soc.*, 2006, **128**, 12; (*e*) E. N. Esenturk, J. Fettinger and B. W. Eichhorn, *J. Am. Chem. Soc.*, 2006, **128**, 9178; (*f*) J. Q. Wang, S. Stegmaier and T. F. Fassler, *Angew. Chem., Int. Ed.*, 2009, **48**, 1998.

9 (*a*) S. C. Critchlow and J. D. Corbett, *Inorg. Chem.*, 1982, **21**, 3286; (*b*) F. Lips, I. Schellenberg, R. Pottgen and S. Dehnen, *Chem.–Eur. J.*, 2009, **14**, 12968; (*c*) S. C. Critchlow and J. D. Corbett, *Inorg. Chem.*, 1985, **24**, 979; (*d*) L. Xu and S. C. Sevov, *Inorg. Chem.*, 2000, **39**, 5383; (*e*) R. C. Burns and J. D. Corbett, *J. Am. Chem. Soc.*, 1982, **104**, 2804; (*f*) R. C. Burns and J. D. Corbett, *J. Am. Chem. Soc.*, 1981, **103**, 2627.

10 M. M. Gillett-Kunnath, A. G. Oliver and S. C. Sevov, *J. Am. Chem. Soc.*, 2011, **133**, 6560.

11 M. M. Gillett-Kunnath, A. Muñoz-Castro and S. C. Sevov, *Chem. Commun.*, 2012, **48**, 3524.

12 J. Rosdahl, T. F. Fassler and L. Kloo, *Eur. J. Inorg. Chem.*, 2005, 2888.

13 *Amsterdam Density Functional (ADF) Code, Release 2012*, Vrije Universiteit, Amsterdam, The Netherlands, 2012, http://www.scm.com.

14 (*a*) J. P. Perdew, K. Burke and Y. Wang, *Phys. Rev. B: Condens. Matter Mater. Phys.*, 1996, **54**, 16533; (*b*) J. P. Perdew, K. Burke and M. Ernzerhof, *Phys. Rev. Lett.*, 1996, **77**, 3865.

15 E. van Lenthe, E. J. Baerends and J. G. Snijders, *J. Chem. Phys.*, 1994, **101**, 9783.

16 (*a*) A. Muñoz-Castro and R. Arratia-Pérez, *Phys. Chem. Chem. Phys.*, 2012, **14**, 1408; (*b*) A. Muñoz-Castro, D. Mac-Leod Carey and R. Arratia-Pérez, *ChemPhysChem*, 2010, **11**, 646; (*c*) A. Muñoz-Castro, *J. Phys. Chem. C*, 2012, **116**, 17197; (*d*) R. Guajardo Maturana, M. Ponce Vargas and A. Muñoz-Castro, *J. Phys. Chem. A*, 2012, **116**, 8737; (*e*) A. Muñoz-Castro, *J. Phys. Chem. A*, 2012, **116**, 520.

17 E. D. Glendening, J. K. Badenhoop, A. E. Reed, J. E. Carpenter, J. A. Bohmann, C. M. Morales and F. Weinhold, *NBO 5.0.*, Theoretical Chemistry Institute, University of Wisconsin, Madison, WI, 2001, http://www.chem.wisc.edu/~nbo5.

18 (*a*) J. Campbell, D. A. Dixon, P. A. M. Helene and G. J. Schrobilgen, *Inorg. Chem.*, 1995, **34**, 5798; (*b*) J. D. Corbett and P. A. Edwards, *J. Am. Chem. Soc.*, 1977, **99**, 3313; (*c*) L. L. Lohr, *Inorg. Chem.*, 1981, **20**, 4229.

19 (*a*) A. Ruiz-Martínez, D. Casanova and S. Alvarez, *Chem.–Eur. J.*, 2008, **14**, 1291; (*b*) S. Alvarez, P. Alemany, D. Casanova, J. Cirera, M. Llunell and D. Avnir, *Coord. Chem. Rev.*, 2005, **249**, 1693; (*c*) J. Cirera, E. Ruiz and S. Alvarez, *Organometallics*, 2005, **24**, 1556.

20 F. Lips and S. Dehnen, *Angew. Chem., Int. Ed.*, 2009, **48**, 6435.